文章编号：1001-9014(2020)02-0137-05

DOI:10.11972/j.issn.1001-9014.2020.02.001

Examination of the durability of interband cascade lasers against structural variations

LIN Yu-Zhe[1,2,3], Jeremy A. MASSENGALE[2,4], HUANG Wen-Xiang[2,4], YANG Rui-Qing[2*], Tetsuya D. MISHIMA[4], Michael B. SANTOS[4]

(1. Laboratory of Solid-State Optoelectronics Information Technology, Institute of Semiconductors, Chinese Academy of Sciences, Beijing 100083, China;
2. School of Electrical and Computer Engineering, University of Oklahoma, Norman 73019, USA;
3. Center of Materials Science and Optoelectronics Engineering, University of the Chinese Academy of Sciences, Beijing 100049, China;
4. Homer L. Dodge Department of Physics and Astronomy, University of Oklahoma, Norman 73019, USA)

Abstract: By studying two interband cascade laser (ICL) wafers with structural parameters that deviated considerably from the design, the durability of the device performance against structural variations was explored. Even with the lasing wavelength blue shifted by more than 700 nm from the designed value near 4.6 μm at 300 K, the ICLs still performed very well with a threshold current density as low as 320 A/cm^2 at 300 K, providing solid experimental evidence of the tolerance of ICL performance on structural variations.

Key words: III-V semiconductors, interband cascade lasers, mid-infrared, quantum wells, type-II heterostructures

PACS: 42.55.Px, 78.67.Pt, 42.70.Hj

带间级联激光器性能对结构变化的耐受性研究

林羽喆[1,2,3], Jeremy A. Massengale[2,4], 黄文祥[2,4], 杨瑞青[2*], Tetsuya D. Mishima[4], Michael B. Santos[4]

(1. 中国科学院半导体研究所 固态光电信息实验室,北京 100083;
2. 俄克拉荷马大学 电子与计算机工程系,美国 诺曼 73019;
3. 中国科学院大学 材料科学与光电工程中心,北京 100049;
4. 俄克拉荷马大学 物理与天文学系,美国 诺曼 73019)

摘要:通过对两种结构参数与设计偏差较大的带间级联激光器(ICL)的研究,探讨了器件性能在结构变化下的耐受性。在300 K时,即使和4.6 μm的设计波长相比蓝移700 nm以上,激光器仍然性能良好,其阈值电流密度低至320 A/cm^2。此研究为带间级联激光器在结构变化方面的耐受性提供了坚实的实验依据。

关 键 词:III-V族半导体;带间级联激光器;中红外;量子阱;II类异质结

中图分类号:TN365, TN248.4 **文献标识码**:A

Introduction

After more than 20 years of efforts since the original proposal of interband cascade (IC) lasers (ICLs) in 1994 at the 7th Inter. Conf. on Superlattices, Microstructures and Microdevices[1], ICLs have been developed with efficient operation to cover a wide range of mid-infrared wavelengths from below 2 to above 11 μm[2-8]. Also, they have been available commercially in recent years[7] for practical applications such as chemical sens-

Received date: 2020-03-02, **revised date**: 2020-03-15 **收稿日期**:2020-03-02,**修回日期**:2020-03-15

Foundation items: Supported by the National Natural Science Foundation of USA National Science Foundation under Grant (ECCS-1931193)

Biography: LIN Yu-Zhe (1990-), male, Shijiazhuang, Ph. D. Research area involves semiconductor laser materials and devices. E-mail: yuzhe.lin@ou.edu

*** Corresponding author**: E-mail: Rui.q.Yang@ou.edu

ing, imaging and industrial processing control. Nevertheless, they are still expensive with very few suppliers and relatively long delivery time. This is partially attributed to the less mature Sb-based III-V materials and related device fabrication technology for ICLs, as well as limited resources for the growth of Sb-based materials compared to more mature InP- and GaAs-based material systems. Consequently, the amount of effort expended in the development of ICLs has been very limited as compared with other semiconductor lasers such as intraband quantum cascade lasers (QCLs)[9]. Many aspects of ICLs have been unexplored or remain in the early phase.

Incomplete understandings or even misconceptions have also affected the development of ICLs. For example, one may perceive that the design and growth of ICLs are difficult due to their complexities, and consequently look for non-cascade approaches[10]. Although a simple and clear argument from an equivalent circuit perspective has already illustrated the superior features of cascade architectures[11], the lack of discussion and examination in the literature about how the device performance of ICLs depends on variations in layer structure parameters may also make some people skeptical. The structural deviations can be minimized by having very stable temperature control of the source cells and substrate. Even so, some unintentional variations in the alloy compositions and layer thicknesses are inevitable due to the range of III-V materials incorporated into the ICL structure and the length of time required to grow it. In this work, by studying devices made from two ICL wafers whose structures unintentionally deviated considerably from the design, we evaluate how well the device performance characteristics can withstand unintentional structural variations. Furthermore, we demonstrate that the device performance can still be quite good even with substantial deviations from the design. Note that the durability that we report for ICLs does not necessarily apply to QCLs, where the fast phonon scattering time is on the order of picoseconds (or even shorter). Since this is comparable to the carrier intraband transit time, the conditions for population inversion are more challenging in QCLs. For ICLs, in contrast, the interband transition time is on the order of nanoseconds-three orders of magnitude longer than the phonon scattering time and intraband transit time in either the conduction or valence band. As such, population inversion can be well established between two interband transition states in ICLs without relying on delicate energy level alignments between different intraband states and the effects of fast phonon-mediated depletion as in QCLs[2].

1 Device design, growth, and fabrication

The ICL structure was designed based on an improved waveguide configuration, which was initially used successfully in InAs-based ICLs[12]. As shown in Fig. 1, the cascade region is sandwiched between two 210-nm-thick GaSb separate confinement layers (SCLs), two 0.9-μm-thick InAs/AlSb superlattice (SL) intermediate

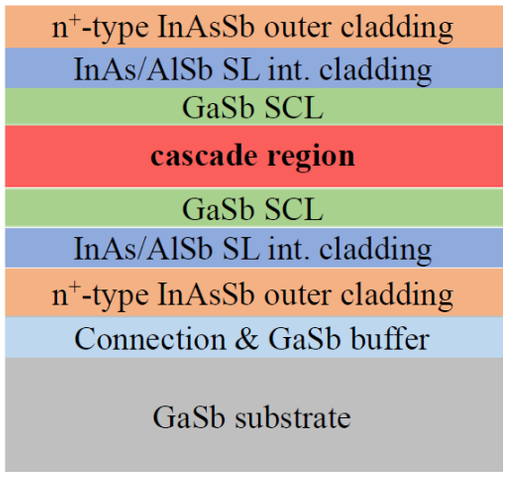

Fig. 1 Schematic drawing of layer structure for GaSb-based ICLs
图1 GaSb基带间级联激光器层结构示意图

(int.) cladding layers, and highly-doped n^+-InAsSb (1.5×10^{19} cm^{-3}) outer cladding layers. In comparison with the InAs-based ICLs[6] where InAs is used for SCLs, because the refractive index of GaSb is substantially higher than that of InAs, the optical confinement factor is enhanced in GaSb-based ICLs when they have the same number of cascade stages. Another benefit with GaSb SCLs is a wide wavelength coverage extended to the shorter wavelengths (e.g. below 3 μm). On the other hand, InAsSb lattice-matched to GaSb needs to be used as the outer cladding layers, which are somewhat more challenging to grow compared to InAs layers. This GaSb-based ICL structure comprises 10 cascade stages, each of which consists of a W-quantum well (QW)[13-14] with one 28-Å-thick $Ga_{0.6}In_{0.4}Sb$ layer sandwiched by two InAs layers (20.5 and 18.5 Å) that were designed to achieve lasing near 4.6 μm at 300 K, similar to what were reported for InAs-based ICLs[6,12].

Following the same ICL design, wafers M368 and M370 were grown by solid-source molecular beam epitaxy (MBE) on 2-inch diameter GaSb (100) substrates. The structural parameters were characterized by using a Philips MRD high resolution x-ray diffraction (XRD) system. Figure 2 shows both the measured diffraction patterns for (004) ω-2θ scans of the two wafers, along with a simulation of the x-ray spectrum. Each pattern shows two sets of superlattice peaks, a narrowly spaced set for the 10 cascade stages (~390 arcsec) and a widely spaced set for the InAs/AlSb superlattice intermediate cladding layers (~3100 arcsec). According to the superlattice peak spacing, the intermediate cladding layers were 7.9% thicker and 0.2% thinner than designed for M368 and M370, respectively. The cascades stages were 5.8% and 6.1% thinner than designed for M368 and M370, respectively. The peak widths for the intermediate cladding layer were ~2 times and ~1.5 times wider for M368 and M370 compared to the simulation. The peak widths for the cascade stages were approximately equal and ~25% wider for M368 and M370, compared to the simulation. The relative narrowness of the peaks indi-

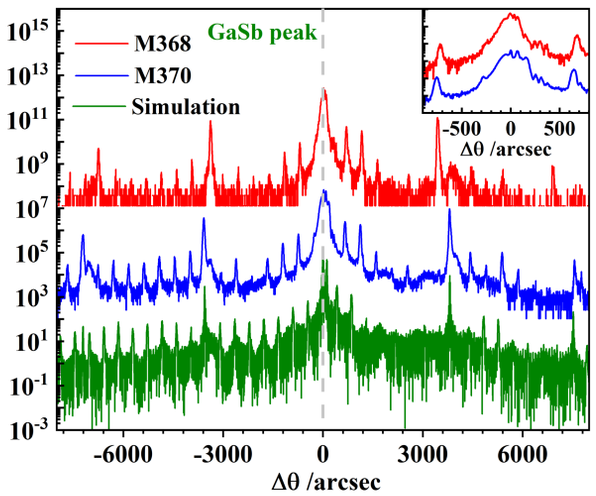

Fig. 2　X-ray diffraction data for wafers M368 (top) and M370 (middle) and a corresponding simulation (bottom) of an ω-2θ scan around the (004) reflection for the GaSb substrate. The scans are offset for clarity
图2　M368(上)、M370(中)和模拟(下)的X射线衍射图,曲线是GaSb衬底上(004)晶面附近所做的ω-2θ扫描(为了清晰起见,曲线已上下平移)

cates that M368 and M370 were not noticeably relaxed.

The wide central peak, shown between Δθ of ±400 arcsec in the inset to Figure 2, includes a peak for GaSb (substrate, buffer, and separate confinement layers), a peak for InAsSb (outer cladding layers), a superlattice peak for the intermediate cladding layers, and two of the closely-spaced (~390 arcsec) peaks for the cascade stages, of which one is a satellite peak. The position of the InAsSb peak was deduced to be approximately -100 arcsec for M368 and M370 because the positions of all the other peaks could be independently determined. This indicated that the compositions of the InAsSb layers were close to the lattice-matched composition.

The two wafers were processed into deep-etched broad-area (150- and 100-μm-wide) mesa stripe lasers by contact photolithography and wet chemical etching. Wafer M370 was cleaved into two pieces that were processed separately. Devices for wafer M370 will be labeled with #1 and #2 for the first- and second-time processes, respectively. The processed wafers were cleaved into laser bars with a length of 1.5 mm and the facets were left uncoated. The laser bars were mounted epilayer side up on copper heat sinks with indium solder and placed on the cold finger of a cryostat for measurements in cw and pulsed modes. In pulsed measurements, the applied current pulse width was 1 μs at a repetition rate of 5 kHz.

2　Device performance and discussion

Broad-area devices made from M368 and M370 lased in cw mode at temperatures up to 220 K (at 3.685 μm) and 228 K (at 3.893 μm as shown by the inset to Fig. 3), respectively. At 80 K, they had slope efficiencies exceeding 400 mW/A from one facet and delivered a cw output power of near 200 mW at 500 mA as shown in Fig. 3. These values are comparable to the best values from previously reported ICLs[6,12,15] with an equal number of cascade stages, the same cavity length, and a lasing wavelength near the designed value. The actual output power and slope efficiency from these ICLs are higher than the above-mentioned values because the measurement calibration included corrections only for the window transmission loss (10%) without accounting for beam divergence. Their threshold voltages V_{th} of 5.0 to 5.4 V at 80 K decreased as their bandgaps became narrower with increasing temperature, as partially reflected by the current-voltage characteristics at different temperatures. At high temperatures, V_{th} increased with temperature (e.g. ~6.4 V at 300 K in pulsed operation) as the threshold current increased more rapidly[6].

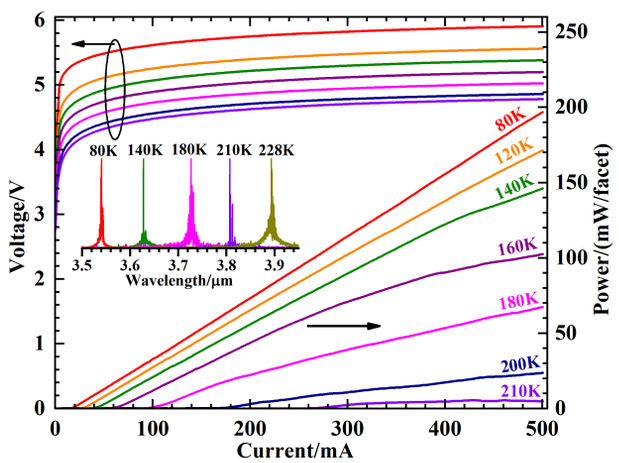

Fig. 3　Current-voltage-light characteristics for a 150-μm-wide device from M370 in cw operation. The inset is the cw lasing spectrum from a 100-μm-wide device at a various heat-sink temperature
图3　150μm条宽M370激光器连续模式下电流电压光功率曲线,插图是100μm条宽器件在不同热沉温度下的连续激光光谱

At 80 K, the lasing wavelength varied from 3.45 to 3.53 μm for devices at different locations in wafer M370, while it ranged from 3.30 to 3.41 μm for devices from wafer M368, implying nonuniformities in the structural parameters across each wafer and between the two wafers. A device from a location near the wafer edge had a lasing wavelength somewhat shorter than a device near the center of the wafer. With an increase in temperature, the lasing wavelengths became longer as shown in Figs. 3 and 4. For example, at 300 K, two 150-μm-wide devices from M370 lased in pulsed mode at 3.87 μm and 3.98 μm (top inset to Fig. 4), while a 100-μm-wide device from M368 lased in pulsed mode at 3.81 μm (bottom inset to Fig. 4).

The lasing wavelengths of these ICLs at 300 K are significantly shorter than the targeted value of 4.6 μm. This is qualitatively consistent with the x-ray diffraction data that indicates that the cascade stages are about 6% thinner than the design value for the two wafers. However, thinner layers in the active QW regions may cause

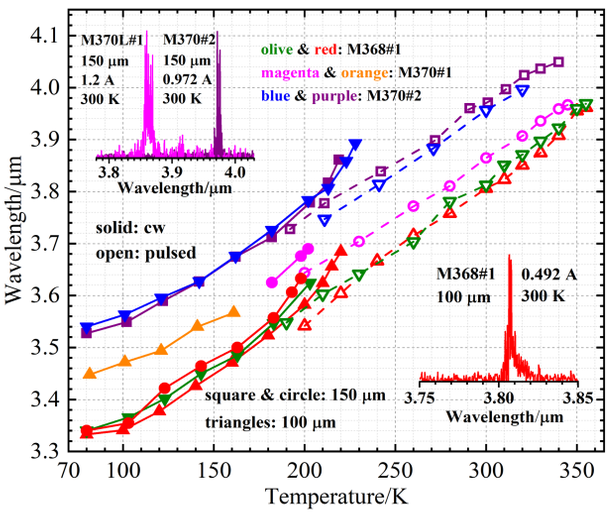

Fig. 4 Lasing wavelength of broad-area ICLs. Inset: pulsed lasing spectra (M368 and M370) at 300 K

图4 宽脊带间级联激光器的激射波长随温度变化趋势,插图是300K脉冲激光光谱(M368和M370)

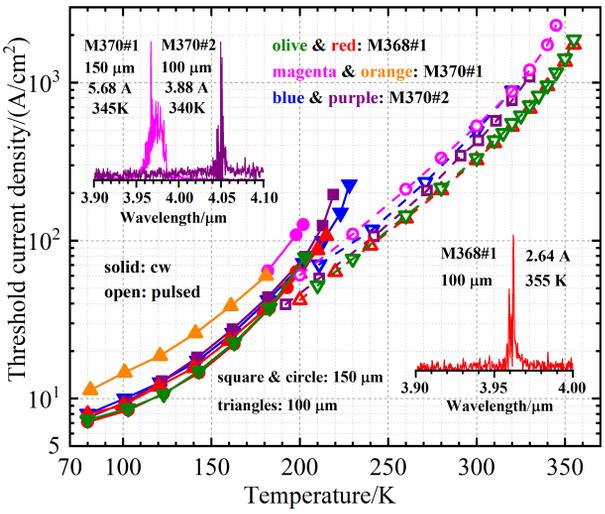

Fig. 5 Threshold current density vs temperature for devices from wafers M368 and M370. Symbols and colors are consistent with those in Fig. 4. Two insets are pulsed lasing spectra for three devices near their thresholds

图5 M368和M370器件的阈值电流密度随温度变化趋势(符号和颜色与图4一致),插图是三个器件接近阈值时的脉冲光谱

about 200 nm blue shifts due to the higher energy levels, but do not completely account for the significant blue shifts of the lasing wavelengths (> 600 nm in M370 and 700 nm in M368). Other factors that may affect the energy levels of QWs and thus lasing wavelengths include possible variations in interface compositions, incorporation of residual As or Sb, and uneven flux fluctuations from different cells during MBE growth. The lasing wavelengths of the ICLs from wafer M368 were somewhat shorter than from wafer M370, but increased with temperature at a slightly faster rate (2.54 nm/K vs. 2.22 nm/K in pulsed operation) as shown in Fig. 4.

Since the two ICL wafers had substantial structural deviations from the design, as reflected from the lasing wavelengths, significant device performance degradation (or even nonfunction) were expected. Nevertheless, devices made from these wafers still performed very well. In pulsed operation, two devices from M368 lased at temperatures up to 355 K near 3.96 μm (lower inset to Fig. 5), while two devices from the first- and second-time processes lased up to 345 K near 3.97 μm and 340 K near 4.05 μm (upper inset to Fig. 5), respectively. Their threshold current densities are comparable to the lowest values (220-300 A/cm^2 at 300 K) reported for ICLs near the design wavelength [3,6,16-17]. For example, a 100-μm-wide device at 300 K from M368 had a threshold current density of 317 A/cm^2 in pulsed mode even though its lasing wavelength (3.81 μm) was blue shifted by more than 700 nm from the targeted wavelength. The threshold current densities of devices from M370 were somewhat higher (e.g. 432 A/cm^2 at 300 K near 3.98 μm). At 80 K, their threshold current densities were from 7.1 to 11 A/cm^2, indicating reasonably high material quality with a low Shockley-Read-Hall recombination. This suggests that the material quality of ICLs can be kept reasonably high even with thickness variations of about 6% during MBE growth.

Their threshold current densities as a function of temperature are shown in Fig. 5, from which the characteristic temperature T_0 can be extracted. T_0 is about 42-48 K in the temperature range from 200 to 320 K, which is typical for mid-IR semiconductor lasers based on interband transitions. It is somewhat surprising that the device performance of these ICLs, in terms of their threshold current densities in a wide temperature range, is remarkably better than that of many early and current mid-IR semiconductor lasers[2,10,18-20], even though the grown structure significantly deviated from the design. This implies that there is still significant room for improving ICL device performance and there are aspects that we do not fully understand. These results at least confirm that carrier transport in ICLs is relatively insensitive to energy level alignments between QWs in the cascade stages. Population inversion can be established relatively easily in a wide range of parameter space based on interband transitions, in contrast to more strict requirements for intraband QCLs where fast phonon scattering between the two involved subbands makes it difficult to achieve population inversion without meeting delicate conditions.

3 Summary and concluding remarks

In summary, the effects of structural variations on ICL device performance were investigated by examining the characteristics of devices made from two wafers with layer thicknesses and compositions that unintentionally deviated considerably from the design. We showed that although the lasing wavelengths of the ICLs were significantly shifted from the targeted value, the device performance was still very good in terms of threshold current density and operating temperature. This is partially attributed to the advantages and flexibility of ICLs based on

interband transitions with a much longer lifetime than the intraband relaxation time via the fast phonon scattering. Also, we demonstrated that the improved plasmon waveguide configuration[12] can be used for ICLs at wavelengths shorter than 4 μm for above room temperature operation. These results suggest important potential for further advancement of ICLs in the 3-4 μm region with a significant reduction of the SL cladding thicknesses, which enhances thermal dissipation and simplifies the MBE growth by minimizing the number shutter movements.

Acknowledgment

The authors acknowledge Lu Li for his help and contributions to device fabrication. LIN Yu-Zhe is grateful to Prof. WH Zheng for her support and advice at the Institute of Semiconductors.

References

[1] YANG R Q. Infrared laser based on intersubband transitions in quantum wells [J]. *Superlattices and Microstructures*, 1995, **17**(1): 77-83.
[2] YANG R Q. Interband Cascade (IC) Lasers, Chap. 12, in *Semiconductor lasers: Fundamentals and applications* [M]. edited by Baranov and E. Tournie Cambridge: Woodhead Publishing Limited, 2013: 487-513.
[3] Vurgaftman I, Weih R, Kamp M, *et al*. Interband cascade lasers [J]. J. *Phys*. D: *Appl. Phys.*, 2015, **48**(12): 123001.
[4] Trofimov I E, Canedy C L, Kim C S, *et al*. Interband cascade lasers with long lifetimes [J]. *Appl. Optics*, 2015, **54**(32): 9441-9445.
[5] LI L, YE H, JIANG Y C, *et al*. MBE-grown long-wavelength interband cascade lasers on InAs substrates [J]. *J. Crystal Growth*, 2015, **425**: 369-372.
[6] YANG R Q, LI L, HUANG W X, *et al*. InAs-based Interband Cascade Lasers [J]. *IEEE J. Selected Topics Quantum Electronics*, 2019, **25**(6): 1200108.
[7] Koeth J, Weih R, Scheuermanna J, *et al*. Infrared Remote Sensing and Instrumentation XXV, San Diego, United States [C]. Proc. SPIE, 2017, **10403**: 1040308.
[8] Shterengas L, Kipshidze G, Hosoda T, *et al*. Cascade Pumping of 1.9-3.3 μm Type-I Quantum Well GaSb-based Diode Lasers [J]. *IEEE Journal of Selected Topics in Quantum Electronics*, 2017, **23**(6): 1-8.
[9] Faist J, Capasso F, Sivco D L, *et al*. Quantum cascade laser [J]. *Science*, 1994, **264**(5158): 553-556.
[10] Jung D, Bank S R, Lee M L, *et al*. Next generation mid-infrared sources [J]. J. *Opt*, 2017, **19**(12): 123001.
[11] YANG R Q, and PEI S S. Novel type-II quantum cascade lasers [J]. *J. Appl. Phys.*, 1996, **79**(11): 8197-8203.
[12] LI L, JIANG Y, YE H, *et al*. Low-threshold InAs-based interband cascade lasers operating at high temperatures [J]. *Appl. Phys. Lett*, 2015, **106**(25): 251102.
[13] Esaki L, CHANG L L, and Mendez E E. Polytype superlattices and multi-heterojunctions [J]. *Jpn*. J. Appl. *Phys.*, 1981, **20**(7): L529-L532.
[14] Meyer J R, Hoffman C A, Bartoli F J, *et al*. Type-II quantum-well lasers for the mid-wavelength infrared [J]. *Appl. Phys. Lett.*, 1995, **67**(6): 757-759.
[15] YANG R Q, LI L, Zhao L H, *et al*. Novel In-Plane Semiconductor Lasers XII, San Francisco, United States [C]. Proc. SPIE, 2013, **8640**: paper 86400Q.
[16] Canedy C L, Warren M V, Merritt C D, *et al*. Quantum Sensing and Nano Electronics and Photonics XIV, San Francisco, United States [C]. Proc. SPIE, 2017, **10111**: 101110G.
[17] Schade A, and Höfling S. Infrared Remote Sensing and Instrumentation XXV, San Diego, United States [C]. Proc. SPIE, 2017, **10403**: 1040305.
[18] YANG R Q. Mid-infrared interband cascade lasers based on type-II heterostructures [J]. Microelectronics J., 1999, **30**(10): 1043-1056; (and references therein.
[19] YANG R Q, Bradshaw J L, Bruno J D, *et al*. Mid-infrared type-II interband cascade lasers [J]. IEEE J. Quantum Electron., 2002, **38**(6): 559-568; (and references therein.
[20] YANG R Q, LI L, JIANG Y, Interband cascade lasers: from original concept to practical devices [J], *Prog. in Physics*(杨瑞青,李路,江宇超,带间级联激光器:从原始概念到实际器件,**物理学进展**) 2014,**34**(4), 169-190.